Surface, Tribological, and Mechanical Characterization of Synthetic Skins for Tribological Applications in Cosmetic Science

Bharat Bhushan,[1] Wei Tang[1,2]

[1]*Nanoprobe Laboratory for Bio- & Nanotechnology and Biomimetics, The Ohio State University, 201 West 19th Avenue, Columbus, Ohio 43210*
[2]*College of Mechanical Engineering, China University of Mining and Technology, Xuzhou, Jiangsu 221116, China*

Received 23 June 2010; accepted 1 September 2010
DOI 10.1002/app.33340
Published online 10 January 2011 in Wiley Online Library (wileyonlinelibrary.com).

ABSTRACT: Synthetic skin as an ideal human-tissue substitute is needed for the research and assessment of hair- and skin-care products. In this study, a systematic study was carried out of the surface, tribological, and mechanical properties of two synthetic skins and rat skin with and without skin-cream treatment with scanning electron microscopy, atomic force microscopy, and a nanoindenter. The film thickness, adhesive force, coefficient of friction, surface roughness, and contact angle of the two synthetic skins and rat skin were comparable. The hardness of one synthetic skin was more similar to rat skin. After treatment with skin cream, the trends of the properties of the two synthetic skins and rat skin were similar. © 2011 Wiley Periodicals, Inc. J Appl Polym Sci 120: 2881–2890, 2011

Key words: atomic force microscopy (AFM); hardness; mechanical properties

INTRODUCTION

When skin has been seriously damaged through burns, the body cannot act fast enough to manufacture the necessary replacement cells. The patient may die from infection and dehydration. Skin grafts constructed from the patient's own skin (autografts) or cadaver skin (allografts) have been developed as a way to repair skin. However, this treatment is still a difficult clinical problem. For a large area burn, autografts cannot work because of the small area of normal skin available to provide replacement for this large area of destroyed skin. Although cadaver allografts are commonly available, rejection and the potential for disease transmission are significant issues. For this reason, there is a great need for the development of synthetic skin to save patients with these extensive burns. Since the first synthetic skin was invented by Burke et al.[1] and successfully used to treat burn victims, many synthetic skin substitutes have been developed and used on patients with full-thickness burns, skin disorders, chronic wounds, and certain forms of cancer.[2–14] The structure and composition of some synthetic skin substitutes are shown in Table I.

In the pharmaceutical and cosmetic industries, skin models are needed for permeation and toxicity studies in the treatment of wounds and for skin replacement in burns.[15,16] In addition to ethical issues, real human skin and animal skin are hard to obtain and expensive and give highly variable results because of individual skin variability. The use of synthetic skin to replace real skin can prevent these problems. Because human skin prevents desiccation and provides protection against environmental hazards (e.g., bacteria, chemicals, UV radiation), synthetic skin should have barrier functions and permeability and show the same reaction to environmental hazards as human skin. The human skin equivalent for these studies is *in vitro* cultured skin that is essentially living skin that is grown *in vitro;* these are also referred to as three-dimensional living skin equivalents. Various types of skin equivalents are commercially available as Episkin (L'Oreal, Lyon, France), SkinEthic (SkinEthic, Nice, France), and Epiderm (MatTek Corp., Ashland, MA). These are epidermis-only models, and attempts have been made to produce full-skin models.[17] Unfortunately, the production of tissue-engineered materials is a complicated process.

In addition to its use for medical applications, synthetic skin is needed as a human-tissue substitute in cosmetic science to study the tribological properties

Correspondence to: B. Bhushan (bhushan.2@osu.edu).
Contract grant sponsor: Chinese Scholarship Council (to W.T.).

TABLE I
Structure and Composition of Some Synthetic Skin Substitutes (Adapted from Jones et al.[11]) [Color table can be viewed in the online issue, which is available at wileyonlinelibrary.com.]

	Schematic representation	Layer
Biobrane™ (Dow Hickam/Bertek Pharmaceuticals, Sugar Land, TX)		1. Silicone. 2. Nylon mesh. 3. Collagen.
Transcyte™ (Advanced Tissue Sciences, Inc., La Jolla, CA)	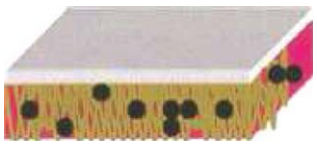	1. Silicone. 2. Nylon mesh. 3. Collagen seeded with neonatal fibroblasts.
Apligraf™ (Organogenesis, Inc., Canton, MA, and Novartis Pharmaceuticals Corp., East Hanover, NJ)	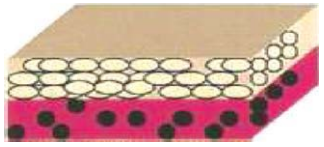	1. Neonatal keratinocytes. 2. Collagen seeded with neonatal fibroblasts.
Dermagraft™ (Advanced Tissue Sciences, LaJolla, California)	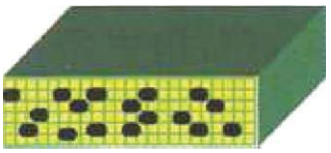	1. Poly(glycolic acid) (Dexon™) or polyglactin-910 (Vicryl™) seeded with neonatal fibroblasts.
Integra™ (Integra Life Science Corp., Plainsboro, NJ)		1. Silicone. 2. Collagen and glycosaminoglycan.
Alloderm™ (LifeCell, Woodlands, TX)		1. Acellular de-epithelialized cadaver dermis.
Epicel™ (Genzyme Tissue Repair Corp., Cambridge, MA)		1. Cultured autologous keratinocytes.
Laserskin™ (Fidia Advanced Biopolymers, Italy; also marketed as Vivoderm™ by ER Squibb & Sons, Inc.)	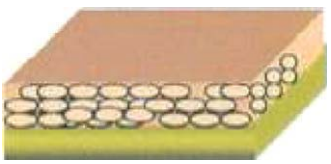	1. Cultured autologous keratinocytes. 2. Hyaluronic acid with laser perforations.
Cadaver allograft (from not-for-profit skin banks)		• Cryopreserved to retain viability. • Lyophilized. • Glycerolized.

of skin and hair during the development and assessment of skin- and hair-care products and the development and assessment of textiles.[18–25] The selected formulation should have film-forming ability, should simulate properties of interest, and respond to cosmetic treatment in a similar way to natural skin. They do not need to be as similar to skin as in medical applications. Various synthetic and natural materials, such as poly(vinyl chloride), polyethylene, polytetrafluoroethylene (Teflon™), poly(methyl methacrylate), polycarbonate, polyurethane, poly(glycolic acid) (Dexon™), polyglactin-910 (Vicryl™),

polyamide (Nylon™), silicon, collagen, cellulose acetate, catgut, and gelatin films have been evaluated as skin substitutes.[11,22,26] A gelatin-based synthetic film (with protein from an animal skin), developed initially at Procter & Gamble, is commercially available as Vitro-Skin™ (IMS, Inc., Milford, CT). It is commonly used for the evaluation of skin-care products, including suntan lotion and cleansing formulations (e.g., refs. 27 and 28). Lir et al.[26] proposed the formulation of a synthetic skin that was molded on a replica of human skin to obtain the appropriate topography.

For tribological applications studies in cosmetic science, it is necessary to develop a systematic methodology for evaluating the surface, tribological, and mechanical properties of synthetic skin that can act as a good reference for researchers. No nanoscale surface mechanical and tribological data exists in literature. It is very useful to bridge the gap between the nanoscale and macroscale data. Particularly, in some studies, nanoscale studies directly simulate the application; for example, the effective and accurate delivery of drugs and genes and the percutaneous absorption of skin-care products occur at the nanoscale. Atomic force microscopy (AFM) and the nanoindenter have emerged over the past few years as viable tools for studying the nanoscale tribological and mechanical properties of materials.[29–32] The properties of interest for tribological applications in cosmetic science include the film thickness, surface roughness, contact angle, hardness, and effective Young's modulus.[22,33–35]

In this study, two relatively inexpensive synthetic skins that were commercially available were chosen for comparison with the rat skin used in previous studies.[35,36] Measurements were also made on the skins after cream treatment. We present a systematic study on the film thickness and adhesive force maps, surface properties (surface topography images, surface roughness, and contact angle), frictional properties (friction force and coefficient of friction), and mechanical properties (hardness and effective Young's modulus). The measurements were performed with an atomic force microscope and a nanoindenter.

EXPERIMENTAL

Skin samples

Two commercially available synthetic skin formulations were selected for the study. Rat skin was also studied to compare its data with that of synthetic skins. Various skins were treated with a skin cream to study their response.

Synthetic skin 1

A commercially available skinlike product, synthetic skin 1 (Dragon Skin), was purchased from Smooth-On, Inc. (Easton, PA).[37] Synthetic skin 1 is a high-performance silicone rubber that is used for a variety of applications that range from the creation of skin effects to medical prosthetics and cushioning applications. Synthetic skin 1 was prepared by the mixture of equal amounts of two components followed by degassing. Then, the mixtures were poured into a casting mold and cured at 65°C for 24 h. After that, synthetic skin 1 was cut into 10 × 10 mm^2 samples and attached to AFM sample pucks with a rapid drying glue (Loctite®). A scanning electron microscopy (SEM) image of the surface of the skin sample is shown in Figure 1.

Synthetic skin 2

Another synthetic skin was produced from the method used by Lir et al.[26] The composition was based on gelatin plasticized by glycerol, polysaccharides, and a mixture of lipids that mimicked the skin's lipid structure and created a hydrophobic surface. We crosslinked it with formaldehyde to improve its hydrolytic stability.

First, a mold with the surface topography of real skin was achieved by a silicone replica technique. A biocompatible silicone liquid (Flexico, a division of Davis Healthcare Services, United Kingdom), originally developed for dental imprints, was purchased from Cuderm Corp. (Dallas, TX).[37] It was applied to the facial skin of a healthy 24-year-old male volunteer for 20 min. When the silicone rubber was peeled off the skin, its topography was a negative replica of the real skin. The replica was cut and glued to a Petri dish for the casting of the synthetic skin.

To prepare the film, gelatin from porcine skin {bloom/gel strength = 175 Bloom [Bloom is a test used to measure the strength of a gel or gelatin. The test determines the weight (in grams) needed by a probe (normally with a diameter of 12.7 mm) to deflect the surface of the gel 4 mm without breaking it. The result is expressed in Bloom (grades)]}, glycerol, and formaldehyde as a 37% water solution were purchased from Sigma-Aldrich. Prolipid 141 (composed of glyceryl stearate, behenyl alcohol, palmitic acid, stearic acid, lecithin, lauryl alcohol, myristyl alcohol, and cetyl alcohol, ISP Global Technologies, Wayne, NJ) was purchased from the Herbarie (Prosperity, SC). Natrosol 250 HHX PHARM was obtained from Hercules. The casting blend was prepared as follows. A 1% gelatin solution was made by the dissolution of 5 g of gelatin in 495 mL of 55°C deionized water, and the pH was adjusted to 9.0 with 1 *M* NaOH. Natrosol® (8 g) and glycerol (0.2 g) were added to the solution and stirred for 2 min. Subsequently, 0.4 g of Prolipid was dissolved in 2 mL of hot ethyl alcohol at 60°C for 5 min and was then mixed with the gelatin solution. Thereafter,

Figure 1 SEM images of the surface of the virgin synthetic skin 1, synthetic skin 2, and rat skin.

2 mL of formaldehyde solution was added and stirred for 1 min. The blend was cast onto the mold and dried at room temperature for 20 h in a chemical hood; this was followed by vacuum drying until a constant weight was reached.[37] The synthetic skin 2 was cut into 10 × 10 mm^2 samples and attached to the AFM sample pucks with rapid drying glue. An SEM image of the surface of the skin sample is shown in Figure 1.

Rat skin

Male rats 8 months old were sacrificed by overdosing with carbon dioxide. The dorsal skin was immediately excised and processed (for details, see refs. 35 and 36). The skin was cut into 10 × 10 mm^2 samples and attached to the AFM sample pucks with the rapid drying glue. A SEM image of the surface of the skin sample is shown in Figure 1.

Cream treatment

There were two categories of skin samples used in the tests: virgin skin and cream-treated skin. The virgin skin was considered to be a baseline specimen. For cream-treated skin, 0.2 mg of a Unilever commercial skin cream, Vaseline Intensive Care Lotion, was applied on a 1-cm^2 area and rubbed throughout the skin surface for 30 s with a cotton swab. For the composition of the cream, see Table II.

Film thickness and adhesive force maps

The experiments were conducted with a commercial AFM system (Dimension Nanoscope IIIa, Veeco, Santa Barbara, CA) under ambient conditions (22°C, RH 35%). A silicon cantilever rotated force-modulation etched silicon probe (Veeco) with a nominal stiffness of 3 N/m was used. The typical radius of a square pyramidal Si tip was less than 10 nm, but blunt tips were preferred for our study so that when the tip compressed the surface, the surface tended to deform elastically instead of being indented (plastic deformation).

The cream film thickness and adhesive force were calculated from the force–distance curve technique (for details, see refs. 35 and 36). In this study, the force curves were collected at the same maximum cantilever deflection of 50 nm (relative trigger

TABLE II
Composition of Common Skin Cream Used in the Study (from Manufacturer Information)

Skin cream	Composition
Common skin cream	Water, glycerin, stearic acid, helianthus annuus seed oil, glycine soja, lecithin, tocopheryl acetate, retinyl palmitate, urea, collagen amino acids, sodium stearoyl lactylate, sodium isostearoyl lactate, mineral oil, sodium PCA, potassium lactate, lactic acid, petrolatum, dimethicone, avena sativa, keratin, glyceryl stearate, cetyl alcohol, methyl palmitate, magnesium aluminum silicate, fragrance, carbomer, stearamide amp, triethanol amine, corn oil, methylparaben, DMDM hydantoin, disodium EDTA, BHT, propylene glycol, titanium dioxide

mode). A 64 × 64 force–distance curve array (a total of 4096 measurement points) was collected over a scan area of 10 × 10 μm^2 with a 4 Hz scan rate for all skin samples. For each force distance curve, there were 128 data points. A custom program coded in MATLAB was used to calculate and display the skin-cream thickness and adhesive force maps.

Surface topography, surface roughness, friction force, and coefficient of friction measurements

The surface topography images of the two synthetic skins and rat skin were taken with SEM (Nova Nanosem 400, FEI, Hillsboro, OR). The samples were first dried with a desiccator. After drying, the samples were carefully mounted on an aluminum stub with double-stick carbon tape. Samples were then introduced into the chamber of the sputter coater, coated with a very thin film (ca. 10 nm) of gold/palladium, and observed in the SEM.

Surface roughness and friction force measurements were performed with AFM. A rotated force-modulation etched silicon probe Si tip with a radius of about 10 nm was used. The surface roughness and friction force images of synthetic skin 1 and rat skin samples were taken at a 120-nN normal load and a 10 μm/s scan velocity over a 30 × 30 μm^2 scan size in contact mode. The surface roughness of synthetic skin 2 was taken over a 30 × 30 μm^2 scan size in tapping mode because the skin was too soft for us to obtain the image in contact mode.

The quantitative measurement of the coefficient of friction was calibrated by the method described by Bhushan.[31,38] The normal load was varied (25–250 nN), and a friction force measurement was taken at each increment. By plotting the friction force as a function of normal load, we obtained an average coefficient of friction from the slope of the fit line of the data.

Contact angle measurement

The contact angle was measured with a Rame-Hart model 100 contact angle goniometer (Rame-Hart Instruments, Netcong, NJ) and water droplets of deionized water. Droplets of about 5 μL (the diameter of a spherical droplet is about 2.1 mm) were gently deposited on the substrate with a micropipette.

Nanoindentation measurement

The nanoindentation experiment was carried out with a Nano Indenter II (MTS Systems Corp.) with a three-sided pyramidal diamond (Berkovich) tip. In this study, the maximum indentation displacement was controlled to 500 nm.

The method for the hardness and elastic modulus determination was based on established methods (for details, see refs. 30 and 39). Briefly, the hardness (H) was calculated from the following equation:

$$H = \frac{P_{\max}}{A} \tag{1}$$

where $P_{\max}$ is the maximum imposed load and A is the projected contact area. The relationship between the contact area and the contact depth was obtained from calibration of the tip with a standard material of known mechanical properties such that the projected contact area was readily obtained from the load–displacement data.

The elastic modulus (E) was analyzed according to the following equations:

$$E = \frac{(1-\nu^2)}{\frac{1}{E_r} - \frac{1-\nu_t^2}{E_t}} \tag{2}$$

where

$$E_r = \frac{\sqrt{\pi}}{2}\frac{S}{\sqrt{A}} \tag{3}$$

The quantity known as the reduced modulus (E_r) was obtained from the ratio of the contact stiffness (S) (obtained from the slope of the unloading curve) and the square root of the contact area, as given in eq. (3). Then, when we knew the modulus of the indenter tip (E_t), the Poisson's ratio of the indenter tip (ν_t), and the Poisson's ratio of the skin (ν), we obtained the elastic modulus from eq. (2). The Poisson's ratio of the skin was assumed to be 0.5; similar assumptions were made by Sanders[40] and Yuan and Verma.[41]

RESULTS AND DISCUSSION

Film thickness and adhesive force maps

Figure 2(a) shows the film thickness and adhesive forces maps and two-dimensional (2-D) profiles at an indicated plane of the two synthetic skins and rat skin with and without skin-cream treatment. Figure 2(b) and Table III show the film thickness and adhesive forces obtained from the maps of the two synthetic skins and rat skin with and without skin-cream treatment.

In the case of virgin skin, the two synthetic skins and rat skin had a similar thin film on the skin surface; this was due to the water and surface compositions. The film thickness and adhesive force values of the two synthetic skins and rat skin were comparable.

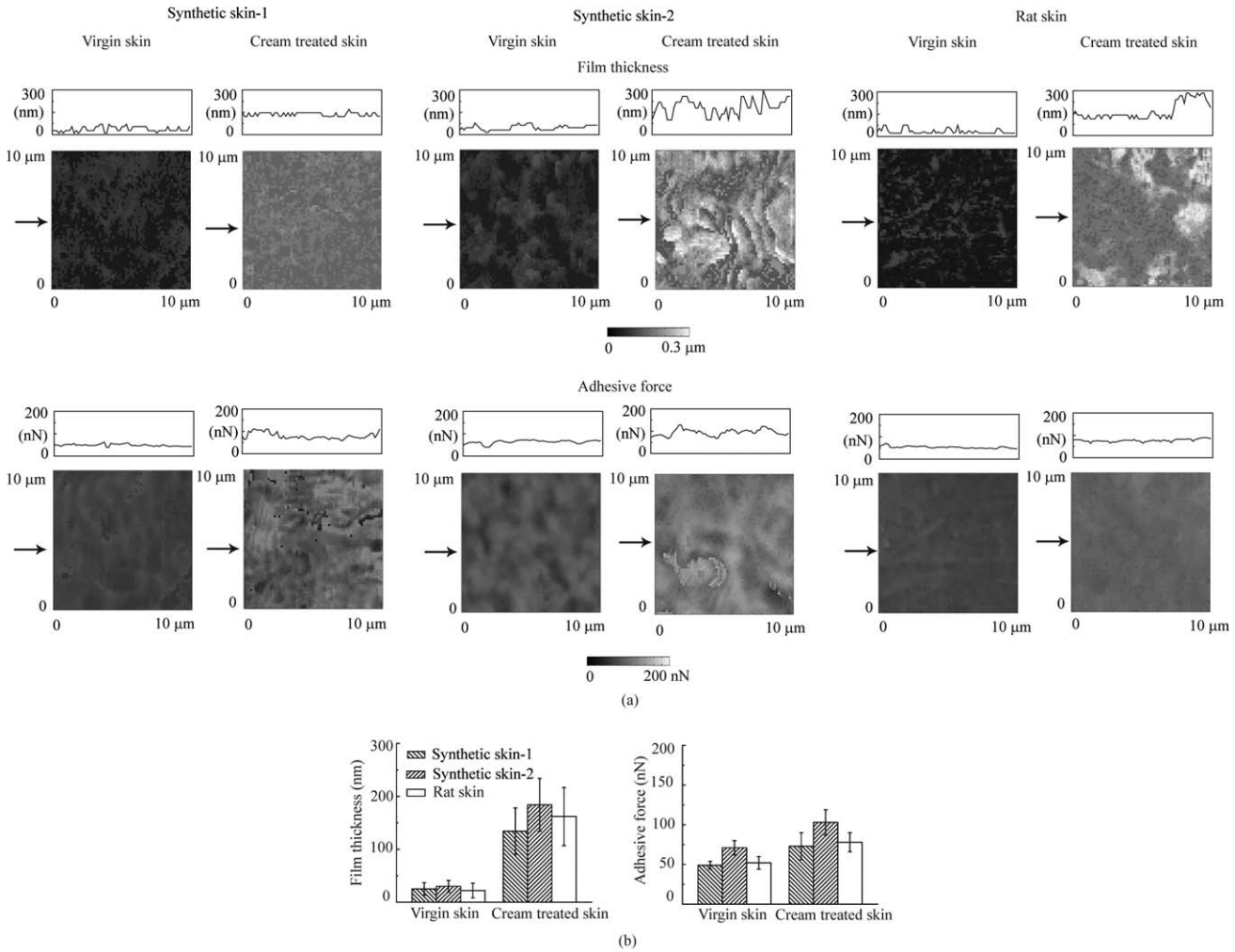

Figure 2 (a) Film thickness and adhesive forces maps for synthetic skin 1, synthetic skin 2, and rat skin with and without cream treatment. Shown above each image is a cross section taken at the position denoted by the corresponding arrows. (b) Film thickness and adhesive forces of the virgin skin and cream-treated skin.

After treatment with skin cream, the film thickness maps showed that the cream film was unevenly distributed on the skin surface, especially for synthetic skin 2 and rat skin. The bright region in the film thickness maps corresponded to a thicker cream film. This means that the adhesive force increased as the film thickness increased. The effect of cream film thickness on the adhesive force has been studied, and the model of the film thickness dependence on the adhesive force was presented by Tang and Bhushan.[36] For the two synthetic skins and rat skin, after treatment with skin cream, the trends of film thickness and adhesive force were same, and both of them increased.

Surface properties

Figure 1 shows the SEM images of the two synthetic skins and rat skin. It shows that the rat-skin surface topography was different from those of the synthetic skins because it was real skin and there were some hair follicles and fractions of hairs on the skin surface. We prepared synthetic skin 1 was prepared by pouring the mixtures into the casting mold and curing them. We prepared synthetic skin 2 by replicating the human face skin. The surface topography of the two synthetic skins were different from rat skin, and there are no hair follicles or hairs present on the skin surfaces.

TABLE III
Film Thickness and Adhesive Force of the Virgin Skin and Cream-Treated Skin Obtained from Maps

	Film thickness (nm)		Adhesive force (nN)	
Skin type	Virgin skin	Cream-treated skin	Virgin skin	Cream-treated skin
Synthetic skin 1	25 ± 12	134 ± 44	49 ± 5	73 ± 14
Synthetic skin 2	30 ± 11	184 ± 50	71 ± 8	103 ± 16
Rat skin	22 ± 14	162 ± 55	52 ± 9	78 ± 15

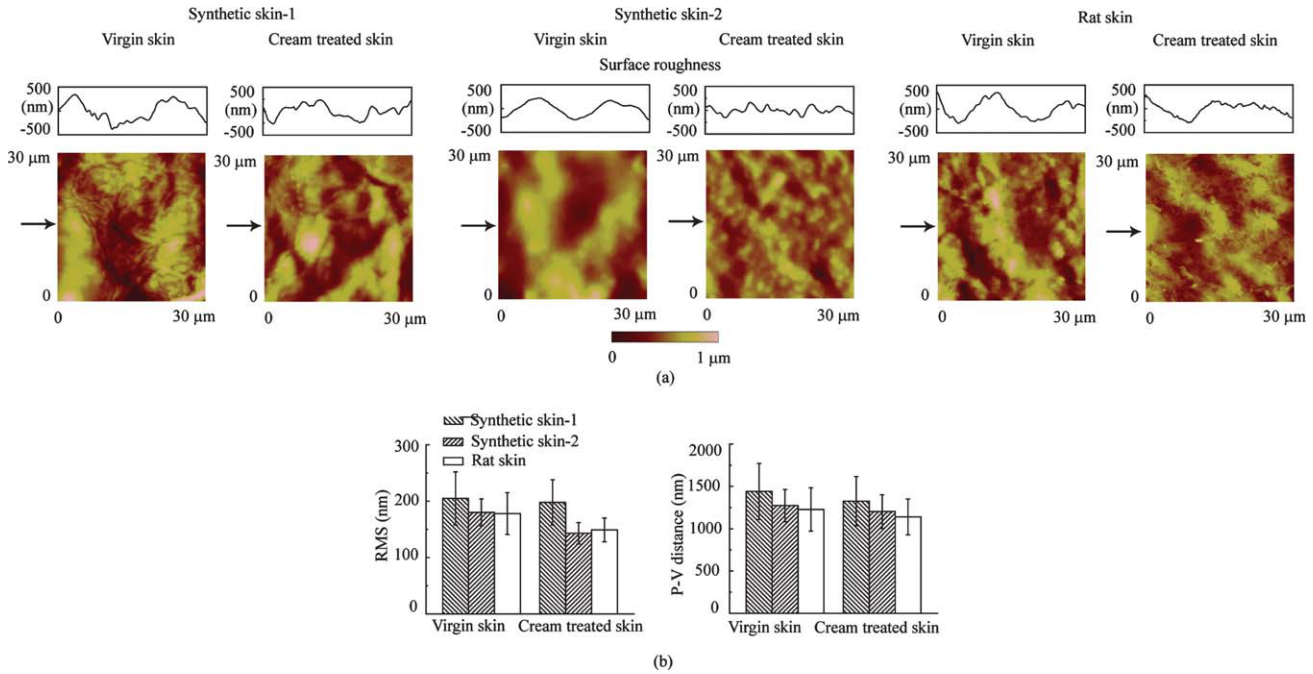

Figure 3 (a) Typical surface roughness AFM images for synthetic skin 1, synthetic skin 2, and rat skin with and without skin-cream treatment. Shown above each image is a cross section taken at the position denoted by the corresponding arrows. (b) RMS and P–V distance of the virgin skin and cream-treated skin. [Color figure can be viewed in the online issue, which is available at wileyonlinelibrary.com.]

Figure 3(a) shows the typical surface roughness AFM images and 2-D profiles at an indicated plane for the two synthetic skins and rat skin with and without skin-cream treatment. The surface roughness statistics on a 30 $\times$30 μm^2 scan size of the two synthetic skins and rat skin with and without skin-cream treatment obtained from the surface roughness AFM images are shown in Figure 3(b) and Table IV. The results show that in the case of virgin skin, the root mean square (RMS) and peak-to-valley (P–V) distance of the two synthetic skins and rat skin were comparable. After treatment with skin cream, the trends of RMS and P–V distance of the two synthetic skins and rat skin were the same, and both of them decreased; this indicated that skin-cream treatment smoothed the skin surface.

TABLE IV
RMS and P–V Distance on a 30 × 30 μm^2 Scan Size of the Virgin Skin and Cream-Treated Skin from Four Sets of Measurements Obtained from the Surface Roughness AFM Images

	Surface roughness statistics			
	RMS (nm)		P–V distance (nm)	
Skin type	Virgin skin	Cream-treated skin	Virgin skin	Cream-treated skin
Synthetic skin 1	205 ± 47	198 ± 40	1442 ± 331	1426 ± 289
Synthetic skin 2	180 ± 24	143 ± 19	1273 ± 191	1201 ± 199
Rat skin	178 ± 37	149 ± 21	1228 ± 256	1040 ± 210

The contact angles of the two synthetic skins and rat skin with and without skin-cream treatment are shown in Figure 4 and Table V. In the case of virgin skin, the contact angles of the two synthetic skins and rat skin were comparable. After treatment with skin cream, the contact angles of the two synthetic skins and rat skin dramatically decreased. The decrease in contact angle indicated that skin cream improved the hydrophilic properties of the skin surface; this helped it to absorb moisture from environment.

Friction force

The typical friction force AFM images and 2-D profiles at an indicated plane for synthetic skin 1 and rat skin with and without skin-cream treatment are

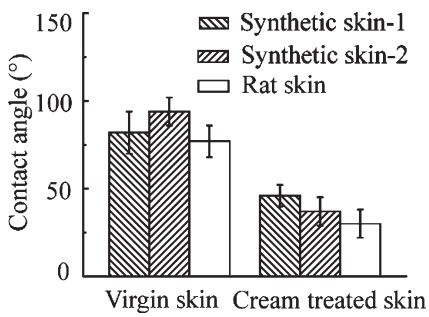

Figure 4 Contact angle of virgin skin and cream-treated skin.

TABLE V
Contact Angle of the Virgin Skin and Cream-Treated Skin from Four Sets of Measurements

Skin type	Contact angle (°)	
	Virgin skin	Cream-treated skin
Synthetic skin 1	82 ± 12	46 ± 6
Synthetic skin 2	94 ± 8	37 ± 8
Rat skin	77 ± 9	30 ± 8

TABLE VI
Coefficient of Friction of the Virgin Skin and Cream-Treated Skin from Four Sets of Measurements

Skin type	Coefficient of friction	
	Virgin skin	Cream-treated skin
Synthetic skin 1	0.050 ± 0.003	0.138 ± 0.027
Synthetic skin 2	0.154 ± 0.062	0.303 ± 0.089
Rat skin	0.087 ± 0.017	0.176 ± 0.032

shown in Figure 5(a). Figure 5(b) and Table VI show the coefficient of friction values of the two synthetic skins and rat skin with and without skin-cream treatment. In the case of virgin skin, the coefficient of friction values of the two synthetic skins and rat skin were comparable. After treatment with skin cream, the friction force values of synthetic skin 1 and the rat skin increased, and the coefficient of friction values of the two synthetic skins and rat skin increased. The reason for the increase in the friction force of the cream-treated skin was the presence of the cream film.[35,36] As the tip slid in the skin-cream film, the viscous friction of the tip with the surrounding cream film led to an increase in the overall friction force.

Nanoindentation

Figure 6(a) shows the typical load–displacement plots for the virgin skin (synthetic skin 1, synthetic skin 2, and rat skin) and cream-treated skin (synthetic skin 1) at 500-nm peak indentation displacement.

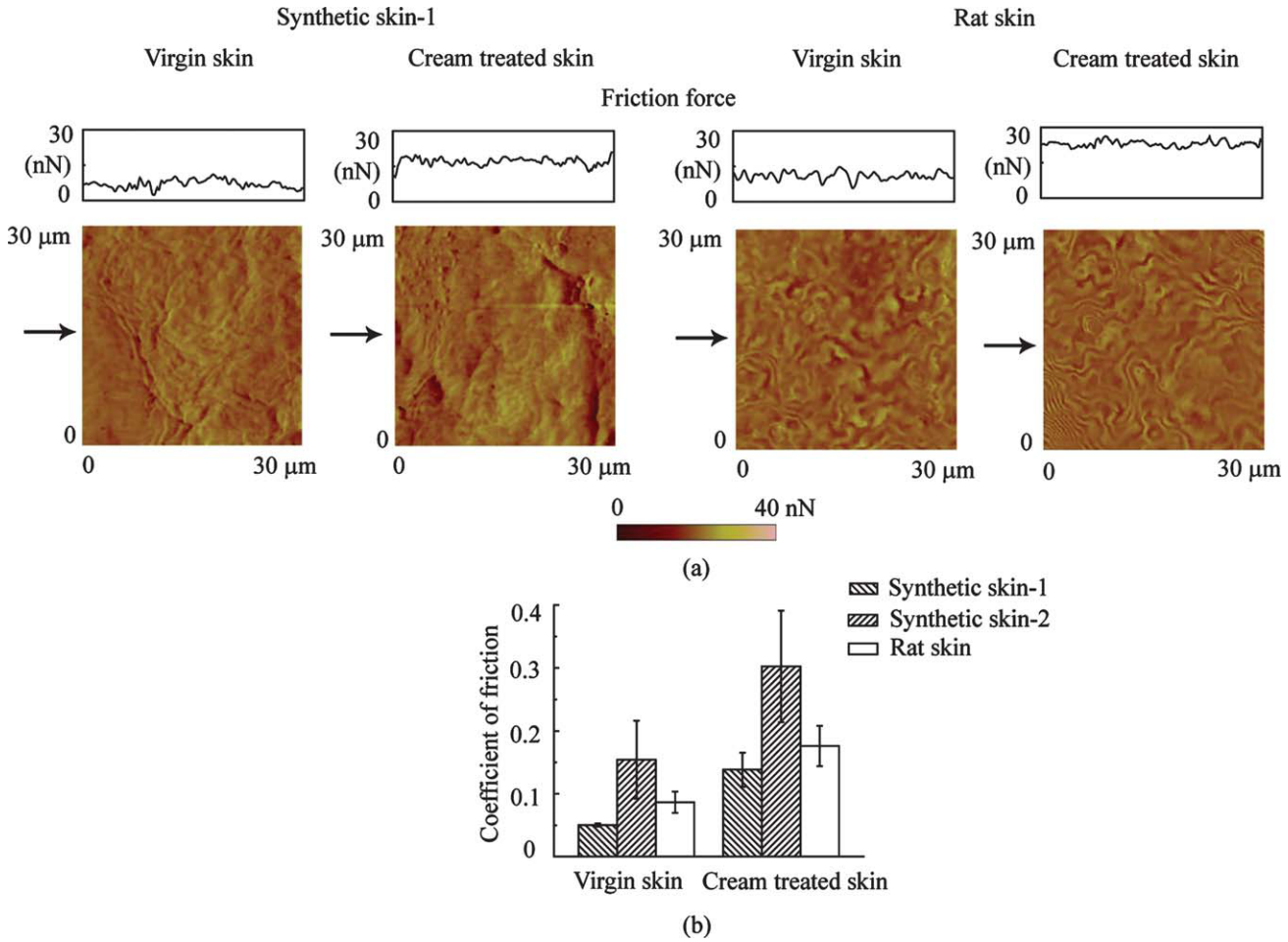

Figure 5 (a) Typical friction force AFM images for synthetic skin 1 and rat skin with and without skin-cream treatment. Shown above each image is a cross section taken at the position denoted by the corresponding arrows. (b) Coefficient of friction of the virgin skin and cream-treated skin. [Color figure can be viewed in the online issue, which is available at wileyonlinelibrary.com.]

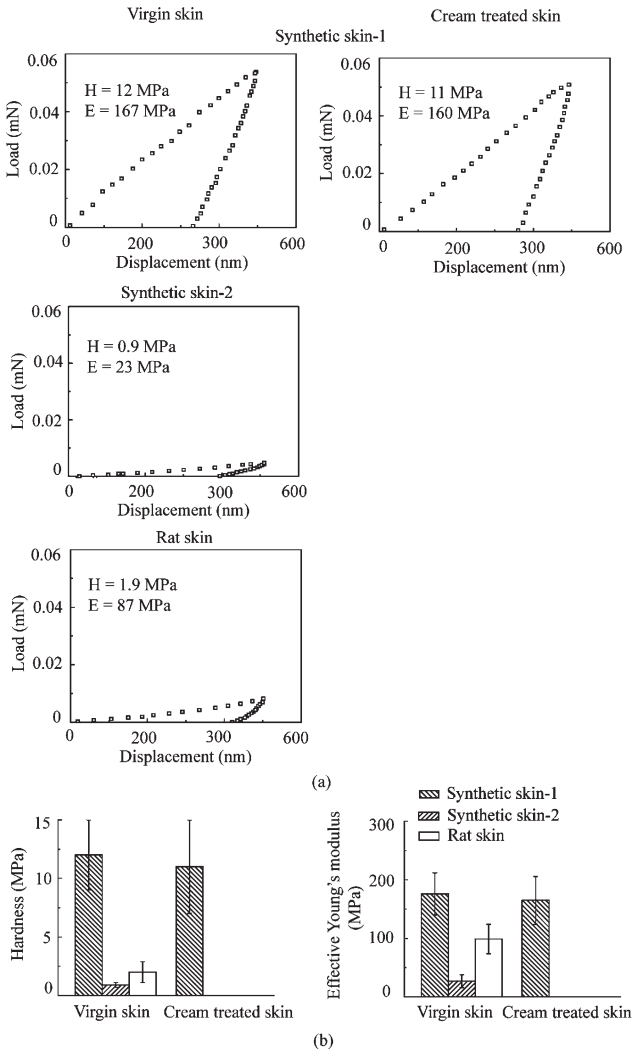

Figure 6 (a) Typical load versus displacement plots for the virgin skin (synthetic skin 1, synthetic skin 2, and rat skin) and cream-treated skin (synthetic skin 1) at a 500-nm peak indentation displacement and (b) hardness and effective Young's modulus of the virgin skin (synthetic skin 1, synthetic skin 2, and rat skin) and cream-treated skin (synthetic skin 1).

TABLE VII
Hardness and Effective Young's Modulus of the Virgin Skin and Cream-Treated Skin Obtained from Three Load–Displacement Curves at a Contact Depth of 500 nm

	Hardness (MPa)		Elastic modulus (MPa)	
Skin type	Virgin skin	Cream-treated skin	Virgin skin	Cream-treated skin
Synthetic skin 1	12 ± 3	11 ± 4	176 ± 36	165 ± 41
Synthetic skin 2	0.9 ± 0.2	—[a]	27 ± 11	—[a]
Rat skin	2 ± 0.9	—[a]	99 ± 25	—[a]

[a] Hardness and effective Young's modulus are not reported because of nanoindenter noise limitations at the depth range tested.

Figure 6(b) and Table VII shows the hardness and effective Young's modulus values of the virgin skin and cream-treated skin. In the case of the virgin skin, the hardness of synthetic skin 1 was higher than those of synthetic skin 2 and rat skin; this indicated its hard texture. The hardnesses of the rat skin and synthetic skin 2 were comparable. The effective Young's modulus of synthetic skin 2 was lower than those of synthetic skin 1 and rat skin. After treatment with skin cream, the hardness and effective Young's modulus of synthetic skin 1 showed a slight decrease; this indicated that the skin cream moistened and softened the skin surface.

CONCLUSIONS

In this article, we presented a systematic nanoscale study of the film thickness and adhesive force maps and surface (surface topography images, surface roughness, and contact angle), adhesion, frictional, and mechanical (hardness and effective Young's modulus) properties of two synthetic skins and rat skin with and without skin-cream treatment with AFM and a nanoindenter. The conclusions from this study are as follows.

Skin cream changed the properties of the skin surface. The presence of the cream film caused an increase in the surface film thickness; this led to an increase in the adhesive force and friction force. The skin cream also reduced the surface roughness, increased the hydrophilic properties of the skin, and softened the skin surface.

The surface topography of the two synthetic skins was different from rat skin, as there were no hair follicles or hairs present on the synthetic skin surface. In the case of virgin skin, the film thickness, adhesive force, coefficient of friction, RMS, P–V distance, and contact angle of the two synthetic skins and rat skin were comparable. After treatment with skin cream, the trends of the properties of the two synthetic skins and rat skin were similar. The film thickness, adhesive force, and coefficient of friction of the two synthetic skins and rat skin increased, and the RMS, P–V distance, and contact angle of the two synthetic skins and rat skin decreased.

In the case of virgin skin, the hardness of synthetic skin 1 was higher than those of synthetic skin 2 and rat skin. The hardnesses of the rat skin and synthetic skin 2 were comparable. The effective Young's modulus of synthetic skin 2 was lower than that of synthetic skin 1 and rat skin.

On the basis of the surface and friction properties, the synthetic skins were good simulations of rat skin. However, the hardness of synthetic skin 2 was comparable to that of rat skin and was a better simulation. After treatment with skin cream, the trends of the properties of the two synthetic skins

and rat skin were comparable. The methodology presented here can act as a good reference for researchers to evaluate the surface, frictional, and mechanical properties of synthetic skins.

The authors thank Carrie Freed of the University Lab Animal Resources of Ohio State University for providing the skin samples. Some of the synthetic skin samples were obtained from Parviz Soroushian and Jue Lu of Technova Corp. The authors give special thanks to Manuel Palacio of Ohio State University for performing nanoindentation testing.

References

1. Burke, J. F.; Yannas, I. V.; Quinby, W. C.; Bondoc, C. C.; Jung, W. K. Ann Surg 1981, 194, 413.
2. Heimbach, D.; Luterman, A.; Burke, J.; Cram, A.; Herndon, D.; Hunt, J.; Jordan, M.; McManus, W.; Solem, L.; Warden, G. Ann Surg 1988, 208, 313.
3. Sheridan, R. L.; Hegarty, M.; Tompkins, R. G.; Burke, J. F. Eur J Plast Surg 1994, 17, 91.
4. Wainwright, D. J. Burns 1995, 21, 243.
5. Gentzkow, G. D.; Iwasaki, S. D.; Hershon, K. S.; Mengel, M.; Prendergast, J. J.; Ricotta, J. J.; Steed, D. P.; Lipkin, S. Diabetes Care 1996, 19, 350.
6. Eaglstein, W. H.; Falanga, V. Clin Ther 1997, 19, 894.
7. Choi, Y. S.; Hong, S. R.; Lee, Y. M.; Song, K. W.; Park, M. H.; Nam, Y. S. Biomaterials 1999, 20, 409.
8. Choi, Y. S.; Hong, S. R.; Lee, Y. M.; Song, K. W.; Park, M. H.; Nam, Y. S. J Biomed Mater Res 1999, 48, 631.
9. Sheridan, R. L.; Tompkins, R. G. Burns 1999, 25, 97.
10. Chou, T.; Chen, S.; Lee, T.; Chen, S.; Cheng, T.; Lee, C.; Chen, T.; Wang, H. Plast Reconstr Surg 2001, 108, 378.
11. Jones, I.; Currie, L.; Martin, R. Br J Plast Surg 2002, 55, 185.
12. Kumar, R. J.; Kimble, R. M.; Boots, R.; Pegg, S. P. ANZ J Surg 2004, 74, 622.
13. Someya, T.; Sekitani, T.; Iba, S.; Kato, Y.; Kawaguchi, H.; Sakurai, T. Proc Nat Acad Sci 2004, 101, 9966.
14. Mansbridge, J. J Anat 2006, 209, 527.
15. Netzlaff, F.; Lehr, C. M.; Wertz, P. W.; Schaefer, U. F. Eur J Pharm Biopharm 2005, 60, 167.
16. Batheja, P.; Song, Y.; Michniak, B.; Kohn, J. Accession No. ADA481863; Defense Technical Information Center: Fort Belvoir, VA, 2006.
17. Curren, R. D.; Mun, G.; Gibson, D. P.; Aardema, M. J. The Toxicologist 2005, 84, 453.
18. Barry, T. R.; David, D.; Michael, R. J Soc Cosmet Chem 1992, 43, 307.
19. Jermann, R.; Toumiat, M.; Imfeld, D. Int J Cosmet Sci 2002, 24, 35.
20. Bhushan, B.; Wei, G.; Haddad, P. Wear 2005, 259, 1012.
21. LaTorre, C.; Bhushan, B. Ultramicroscopy 2005, 105, 155.
22. Bhushan, B. Prog Mater Sci 2008, 53, 585.
23. Gerhardt, L. C.; Schiller, A.; Müller, B. Tribol Lett 2009, 34, 81.
24. Nonomura, Y.; Fujii, T.; Arashi, Y.; Miura, T.; Maeno, T.; Tashiro, K.; Kamikawa, Y.; Monchi, R. Colloids Surf B 2009, 69, 264.
25. Horiuchi, K.; Kashimoto, A.; Tsuchiya, R. Tribol Lett 2009, 36, 113.
26. Lir, I.; Haber, M.; Dodiuk-Kenig, H. J Adhes Sci Technol 2007, 21, 1497.
27. Turner, R. B.; Biedermann, K. A.; Morgan, J. M.; Keswick, B.; Ertel, K. D.; Barker, M. F. Antimicrob Agents Chemother 2004, 48, 2595.
28. Wakefield, G.; Stott, J. J Cosmet Sci 2006, 57, 385.
29. Binnig, G.; Quate, C. F. Phys Rev Lett 1986, 56, 930.
30. Oliver, W. C.; Pharr, G. M. J Mater Res 1992, 7, 1564.
31. Nanotribology and Nanomechanics, 2nd ed.; Bhushan, B., Ed.; Springer: Heidelberg, Germany, 2008.
32. Springer Handbook of Nanotechnology, 3rd ed.; Bhushan, B., Ed.; Springer, Heidelberg, Germany, 2010.
33. Chen, N.; Bhushan; B. J Microsc 2006, 221, 203.
34. Lodge, R. A.; Bhushan, B. J Vac Sci Technol A 2006, 24, 1258.
35. Tang, W.; Bhushan, B.; Ge, S. J Microsc 2010, 239, 99.
36. Tang, W.; Bhushan, B. Colloids Surf B: Biointerfaces 2010, 76, 1.
37. Soroushian, P.; Lu, J. Technova Corp., Lansing, MI. Personal communication, 2009.
38. Bhushan, B. Handbook of Micro/Nanotribology, 2nd ed.; CRC: Boca Raton, FL, 1999.
39. Bhushan, B.; Li, X. Int Mater Rev 2003, 48 125.
40. Sanders, R. Pflügers Arch 1973, 342, 255.
41. Yuan, Y.; Verma, R. Colloids Surf B 2006, 48, 6.